



HOMO-LUMO Energies and Geometrical Structures Effecton Corrosion Inhibition for Organic Compounds Predict by DFT and PM3 Methods

Ahmed H. Radhi¹, Ennas AB. Du², Fatma A. Khazaal³, Zaid M. Abbas⁴, Oday H. Aljelawi⁵, Salam D. Hamadan⁴, Haider A. Almashhadani⁶ and Mustafa M. Kadhim^{4*}

Abstract

A theoretical study on corrosion inhibitors was done by quantum calculations includes semi-empirical PM3 and Density Functional Theory (DFT) methods based on B3LYP/6311++G (2d,2P). Benzimidazole derivative (oxo(4-((phenylcarbamothioyl) carbamoyl)phenyl) ammonio) oxonium (4NBP) and thiourea derivative 2-((4-bromobenzyl)thio) -1H-benzo[d] imidazole (2SB) were used as corrosion inhibitors and an essential quantum chemical parameters correlated with inhibition efficiency, EHOMO (highest occupied molecular orbital energy) and ELUMO (lowest molecular orbital energy). Other parameters are also studied like energy gap [ΔE (HOMO-LUMO)], electron affinity (EA), hardness (Δ), dipole moment (μ), softness (S), ionization potential (IE), absolute electron negativity (χ), and global electrophilicity index (ω) respectively. Mulliken population was also essential to determine a local reactivity by indicating reactive centers and identifying a potential nucleophilic and electrophilic attacks sites. The adsorption of compounds is also discussed with the bonds length, the angles, and tetrahedral of molecules. The 2SB best from 4NBP as corrosion inhibitors according to theoretical and experimental proving. Predicated.

37

Key Words: Inhibition, DFT, Adsorption, PM3, Corrosion.

DOI Number: 10.14704/nq.2020.18.1.NQ20105

NeuroQuantology 2020; 18(1):37-45

Introduction

Quantum Mechanics Calculation Theory consists of multiple programming languages, Parametric Method 3 (PM3) is considered one of these languages [1-3]. PM3, which is developed by Dewar and coworkers, is very useful in the calculation of molecular cloning of energies, the replication of molecular structures, and the interpretation of the chemical reaction [4,5]. DFT method is able to predict a wide range of molecular characteristics

like molecular weight infrared, chemical concepts that are generally used on a big scale for characterization of the chemical reaction [6,7], electrical hardness or softness [8], metal surface corrosion, and etc. [9,10]. The corrosion inhibitor is one of the most efficient and economical techniques used to protect the outer surface of metals commonly used in industry from the environmental impact [11].

Corresponding author: Mustafa M. Kadhim

Address: ¹Department of Nursing, AL-Suwaria Technical Institute, Middle Technical University, Iraq; ²Chemistry Department, College of Science for Women, Baghdad University, Baghdad, Iraq; ³Department of Biology, College of Education for Pure Sciences, Wasit University, Wasit, Iraq; ⁴Department of Chemistry, College of Science, Wasit University, Wasit, Iraq; ⁵Department of Chemistry, College of Science, Baghdad University; ⁶Dentistry Department, AlRasheed University College, Baghdad, Iraq.

^{4*}E-mail: Mustafa_kut88@yahoo.com

Relevant conflicts of interest/financial disclosures: The authors declare that the research was conducted in the absence of any commercial or financial relationships that could be construed as a potential conflict of interest.

Received: 18 December 2019 **Accepted:** 12 January 2020



Chemical compounds containing heterogeneous atoms are not bound together, including nitrogen, sulfur, oxygen, and phosphorus[12], the chemical activity of these atoms toward neighboring molecules of the metal surface is very effective via interaction by adsorption[13–15].

The benefit of having effective polar functional groups as a reactive sites is to lead to the state of stability of the adsorption process[16,17]. Benzimidazole is a heterocyclic organic aromatic compound with a bicyclic composition consisting of fused benzene and imidazole rings, the hydrogen atoms on the rings may be replaced by other groups or atoms to serve as inhibitor agent [18,19]. In other words, benzimidazole derivatives are great corrosion inhibitors for metals in acidic solution; the inhibition amount differs with substituent groups, and the imidazole ring substituent positions. The testing shows that thiourea derivatives are cathodic-type inhibitors, which deters the reduction of protons and therefore indirectly the oxidation of the surface[20].

Some of the other parameters mentioned in this work should be included, such as the effect of solvent molecules, the nature of the surface, the absorption sites of metal atoms or oxide sites or vacant seats, the competitive adsorption of various other chemical species during the liquid phase and the solid phase[21]. In this study, quantum mechanical calculations of the approximate semiempirical theory PM3 and Density Functional Theory DFT (B3LYP) based on 6-311++G (2d,2p) were theoretically selected as better corrosion inhibitors using the Gaussian-09 program to study physical characteristics and adsorption behavior. Because of the the huge complication of such kind of theoretical calculations that be needed to take in a consideration the nature of metal surface, inhibitor chemistry and solvent molecules active site, so that the corrosion inhibition processes will not be predicted in an accurate way.

Results and Discussion

Molecular Geometry

By using Chem Draw of Mopac program The compounds were built and equilibrium geometries calculated by Gaussian 09 package[22]. The optimized geometries were calculated by semiempirical method PM3 and Density Functional Theory (DFT) using (B3LYP) with a 6-311++G (2d, 2p) level[23,24]. The final

geometries of 4NbP and 2SB designed according to a correct method DFT are given in (Figure1).

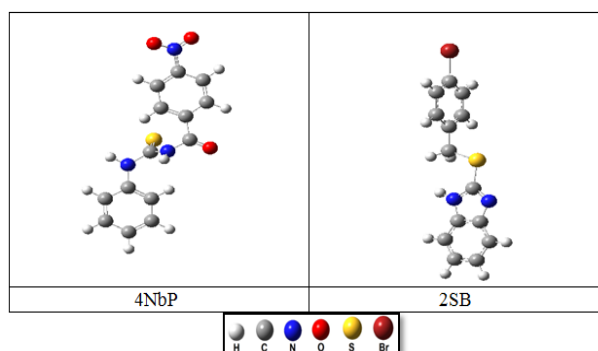
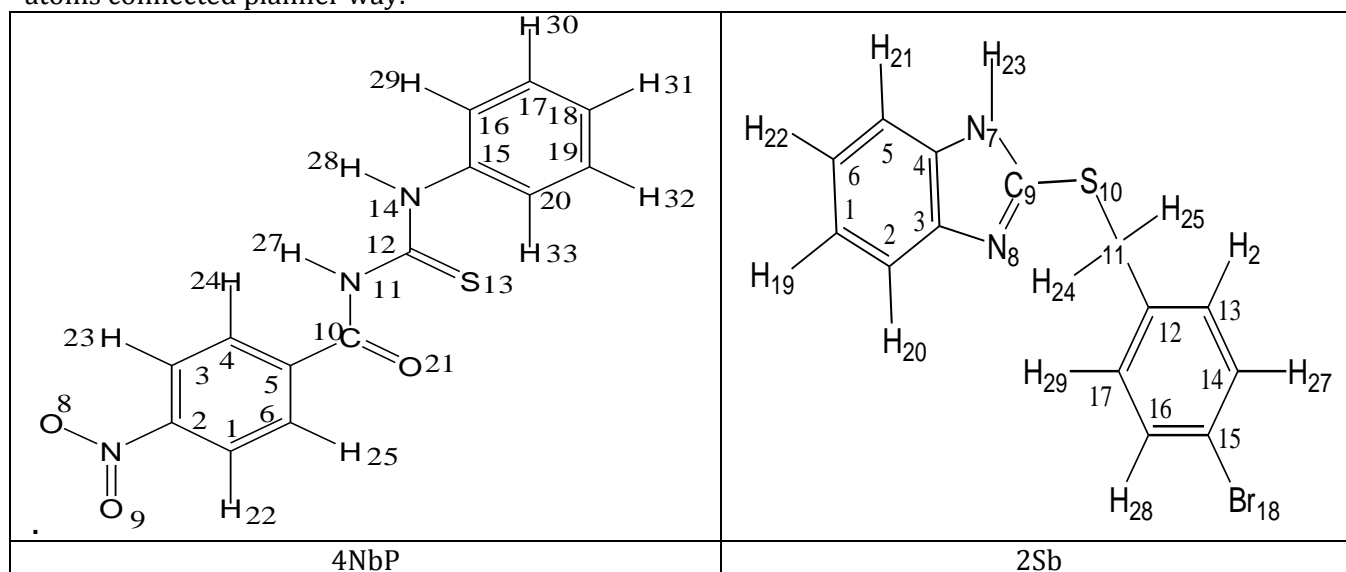


Figure 1: Equilibrium geometry of the inhibitors molecules considered by using DFT (B3LYP/6-311++G (2d,2p)) methods

The difference of atoms' arrangement will lead to a difference in the computational results involves significant modifications on the structural parameters such as bond angles, bond distances, and dihedral angles of the studied inhibitors (Table 1 and Table 2). If a comparison made between the similar bond lengths, the geometrical structure of 4NbP shows a difference in the bond length with about (0.0007-0.3561 Å), and that difference is happened due to the large bulky volume of atoms (Table 1). Moreover, the under investigation molecule 4NbP are not planar and its adsorption on a metallic surface is not easy upon the resulted values of the molecule angles H23-C1-C6, N-C1-C2, O8-N-O9, C2-N-O8, C5-C10-N11, C12-N11-H27 (Table 1). The values of trans dihedral angles (H31-C18-C19-C20, H32-C28-C20-C16, O21-C10-N11-H27, N11-C10-C5-C4, O21-C10-C5-C6, H27-N11-C12-N14, O8-N-C2-C1) atoms and cis dihedral angles (H31-C18-C19-H32, H32-C19-C20-H33, H33-C20-C16-H34, O21-C10-C5-C4, N11-C10-C5-C6, H28-N14-C12-N11) atoms show that the molecule 4NbP is not a planar in this part of the molecule shown above. The 2SB molecule with bond lengths different with about (0.1-0.01 Å) at 2C-1C, C1-6C, 6C-5C, 19H-1C, 3C-2C, 5C-12H in addition to differenceless in the other bond lengths make the structure, not planar as shown in (Table 2 and Table 3). Trans dihedral angles H28C16C15C14, Br18C15C16C17, H27C14C15C16, H28C16C17C12, H26C13C12C17, N1C9N3H23, H23N7C4C3 and cis dihedral angles H28C16C15Br18, Br18C15C14H27, H29C17C16H28, H26C13C12C11, C4C3N3N1, C2C3C4C5 are close to standard angles for planar structure (180, 0 Å) sequentially. According to these results, 2SB is not a fully planar but it adsorbs in some areas in an excellent way where

atoms connected planner way.

**Figure 2.** Label of 4NbP and 2Sb inhibitors compounds.**Table 1.** Calculated geometrical structure for 4NbP molecule by using the DFT method

Description of Bond length	Bond length (Å)	Description angle (deg)	Angle (deg)	Description of Dihedral angle (deg)	Dihedral angle (deg)
H34-C16	1.08145	H31-C18-C19	120.04	H31-C18-C19-H32	-0.201
H33-C20	1.08223	H31-C18-C17	119.09	H32-C19-C20-H33	0.116
H32-C19	1.0802	H32-C19-C20	120.40	H33-C20-C16-H34	-0.689
C18-C17	1.38885	H34-C16-C20	120.27	H28-N14-C12-N11	-7.549
C15-N14	1.41899	C15-C17-H30	120.39	H27-N11-C10-C5	-3.329
C12-N14	1.33577	H28-N14-C12	118.22	C10-C5-C4-H25	-0.224
C12-S13	1.67297	N14-C12-S13	125.40	H25-C4-C3-H24	0.626
C12-N11	1.40241	S13-C12-N11	118.99	H24-C3-C2-N	0.069
H27-N11	1.00651	C12-N11-H27	111.96	C3-C2-N-O8	31.930
C10-N11	1.37577	C10-N11-C12	129.01	C3-C2-N-O9	-33.612
O21-C10	1.22506	C10-N11-H27	119.01	N-C2-C1-H23	0.692
H31-C18	1.08154	H33-C20-C16	119.33		
H30-C17	1.07989	H32-C19-C18	120.46		
C16-C20	1.38622	H33-C20-C19	120.09		
C20-C19	1.39360	H33-C20-C16	119.33		
C17-C15	1.39225	H34-C16-C15	119.60		
C18-C17	1.39392	S13-C12-N11-H27	4.431		
C16-C15	1.39836	C12-N11-C10-O21	-3.417		
N14-H28	1.01624	N11-C10-C5-C6	-23.362		



Table 2. Calculated geometrical structure for 2Sb molecule by using the DFT method.

Description of Bond length	Bond length (Å)	Description angle (deg)	Angle (deg)	Description Dihedral angle (deg)	Dihedral angle (deg)
2C-1C	1.388	H28C16C15	120.448	H28C16C15Br18	-0.131
3C-2C	1.394	C16C15Br18	119.468	Br18C15C14H27	0.130
4C-3C	1.409	Br18C15C14	119.469	H27C14C13H20	0.271
C4-C5	1.389	C15C14H27	120.446	H26C13C12C11	0.155
1C-6C	1.403	H27C14C13	120.425	C11C12C17H29	-0.099
19H-1C	1.081	C14C13H26	119.152	H29C17C16H28	-0.325
C2-H20	1.080	H26C13C12	119.828	C17C12C11H24	30.804
C3-N8	1.387	C13C12C11	120.678	C13C12C11H25	-28.246
C4-N7	1.388	C11C12C17	120.674	H24C11S10C9	58.223
6C-5C	1.390	C12C17H29	119.809	H25C11S10C9	-61.047
-5CH21	1.0814	H29C17C16	119.180	H23N3C9O10	0.317
C6-H22	1.0810	C17C16H28	120.415	N1C9N3C4	-0.147
N7-H23	1.002	H24C11C12	110.556	C4C3N3N1	-0.029
N7-C9	1.378	H25C11C12	110.370	C2C3C4C5	0.028
N8-C9	1.304	H24H25C11	109.664	H20C2C3N1	-0.109
C9-S10	1.761	C12C11S10	108.881	H21C5C4N3	0.099
C11-S10	1.850	H25C11S10	108.769	H21C5C6H22	0.006
H25-C11	1.0886	H24C11S10	108.551	H22C6C1H19	-0.025
C11-C12	1.504	C11S10C2	102.233	H19C1C2H20	-0.014
C11-H24	1.0885	N1C2S10	121.626	H28C16C15C14	-179.966
C11-C12	1.395	N3C2S10	125.112	Br18C15C16C17	179.764
C13-C14	1.389	C2N3H23	126.905	Br18C15C14C13	179.72Sb
C14-C15	1.3876	C2N1C5	105.218	H27C14C13C12	-179.751
C15-C16	1.3878	C2N3H23	126.905	H27C14C15C16	179.965
C16-C17	1.3896	H23N3C4	126.457	H28C16C17C12	179.732
C12-C17	1.395	N3C4C5	104.656	H29C17C16C15	179.609
C17-H29	1.082	C5C4C9	122.685	H26C13C12C17	-179.553
C16-H28	1.079	C4C9H21	122.110	C13C12C11H24	-149.753
C15-Br18	1.915	C9C8H22	119.276	H25C11C12C17	152.312
C14-H27	1.079	H22C8C7	119.361	S10C11C12C13	91.077
C13-H26	1.082	C8C7H19	119.032	N1C9N3H23	-179.139
C13-C14	1.389	C2N3H23	126.905	H23N7C4C3	179.051

Molecular Reactivity

Limits orbital theory is very useful in predicting adsorption inhibitor molecules and interact with the metals. Frontier molecular orbital (FMO) can be delivera theoretical results easily, according to the value of the energy gap between E_{HOMO} and E_{LUMO} ($\Delta E = E_{\text{LUMO}} - E_{\text{HOMO}}$). The energy HOMO (E_{HOMO}) refers to the ability to donor of electron to an acceptor; the high morals of E_{HOMO} tendency to donate electrons to the acceptor with low energy molecular orbital empty. The parameter energy LUMO (E_{LUMO}) refers to the ability to accept an electron of the molecule. This is the lowest value higher electron-compliant capability. hole energy between the

in the description of the molecular activity, so when the energy gap decreased, improving the efficiency of the inhibitor [25]. The ionization energy (IE) and electronic affinity (EA) is related to the HOMO energy and the LUMO energy as follows [26]:

IE (Ionization potential) = $-E_{\text{HOMO}}$
amount of energy essential (IE) for removing the electron of an atom. The low ionization energy gives great efficiency for inhibition.

EA (Electron affinity) = $-E_{\text{LUMO}}$
amount of free energy (EA) when the electron is supplementary to a neutral atom. The superior value of electron means less stability and gives high efficiency for inhibition.



Hardness (η) has been distinct as the second unoriginal of the E. measures the stability and the molecular reactivity [27].

$$\eta \text{ (Hardness)} = (IE - EA) / 2$$

$$\chi \text{ (Electronegativity)} = -\mu = (IE + EA) / 2$$

This rate is related to the (HOMO) and the (LUMO) of energy. The small value of electronegativity meaning great inhibitor efficiency.

the global hardness is the opposite of The global softness (S) [28]. Softness another parameter to measure the molecular stability and reactivity

$$S \text{ (global softness)} = 1 / \eta$$

by Parr the Global electrophilicity index (ω) are introduced [29], the stabilization is measured after a molecule accepts an extra number of electron. Suitable inhibitor with a lower value of the global electrophilicity index.

$$\text{The Global of electrophilicity index } (\omega) = (-\chi)^2 / 2\eta$$

Whereas, the amount of the electrons transferred (ΔN) from the inhibitor to the carbon steel surface was also indicated by using the theoretical values of 7.0 eV mol⁻¹ and 0.0 eV mol⁻¹ for mild steel, respectively. The ΔN

values are linked to inhibition efficiency [30], which is shown in (Table 4 and Table 6) according to results from PM3 and DFT. While, the highest inhibition efficiency contemplates experimentally for 2Sb electrons flow from lower χ to higher χ until the chemical potentials become equal. For example, two systems Fe and inhibitor are brought together to obtain (ΔN), electrons will flow from an inhibitor to Fe and this will lead to (ΔN) also calculated by using the equation [31]:

$$\Delta N \text{ (Electron transferred)} = (\chi_{Fe} - \chi_{inhib.}) / [2 (\eta_{Fe} + \eta_{inhib.})]$$

Where, χ_{Fe} denote the absolute electronegativity of iron and χ_{inh} electronegativity of inhibitor molecule η_{Fe} and η_{inh} denote the absolute hardness of iron and the inhibitor molecule, respectively. The dipole moment (μ in Debye) is another significant electronic parameter its product from uniform distribution charge on the atoms and the distance between the two bonded atoms. High values of dipole moment are reported to facilitate adsorption and therefore inhibition by influencing the transport process through the adsorbed layer, the inhibition efficiency increases with dipole moments values [32]. The dipole moments of 4NbP and 2Sb are (4.47913, 2.686 Debye), for PM3 method and (0.7028, 4.3139 Debye) for DFT method Tables 3, 5 respectively. Metallic surface

and these compounds probably indicate strong dipole-dipole interactions. The superior value of the premeditated (μ) and the other limits efficiency of the inhibitor molecule 2Sb enumerates its better inhibition efficiency than 4NbP. DFT calculations Tables 5, 6 even so PM3 calculations, Tables 3, 4.

Table 3. PM3 calculated certain physical properties for the inhibitors molecules at the equilibrium geometries.

Inhib. b.	M. formula M. wt. (gm/mol)	E _{HOMO} (eV)	E _{LUMO} (eV)	$\Delta E_{HOMO-LUMO}$ (eV)	μ (Debye)
4NbP	319.218 gm/mol	-9.005	-1.525	-7.48	2.686
2Sb	316.334 gm/mol	-8.75	-0.868	-7.88	4.47913

Table 4. Quantum chemical parameters for the inhibitor molecules as calculated using the PM3 method.

Inhib.	IE (eV)	EA (eV)	η (eV)	χ (eV)	S (eV)	ω (eV)	ΔN
4NbP	8.75	0.868	3.941	4.80	0.253	2.934	0.277
2Sb	9.005	1.525	3.74	3.74	0.267	3.705	0.435

Table 5. DFT calculated for some physical properties of the 4NbP and 2Sb inhibitors molecules at the equilibrium geometries.

Inhib.	M. formula M. wt. (gm/mol)	E _{HOMO} (eV)	E _{LUMO} (eV)	$\Delta E_{HOMO-LUMO}$ (eV)	μ (Debye)
4NbP	319.218	-6.0402	-2.922	-3.1174	0.7028
2Sb	316.334	-5.9773	-1.358	-4.6184	4.3139

Table 6: Quantum chemical parameters for the 4NbP and 2Sb inhibitors molecules calculated by using the DFT method.

Inhib.	IE (eV)	EA (eV)	η (eV)	χ (eV)	S (eV)	ω (eV)	ΔN
4NbP	6.0402	2.9228	1.5587	4.4815	0.6415	6.4422	0.807
2Sb	5.9773	1.358	2.3092	3.6681	0.4330	2.9133	0.7214

Local reactivity of the two inhibitors

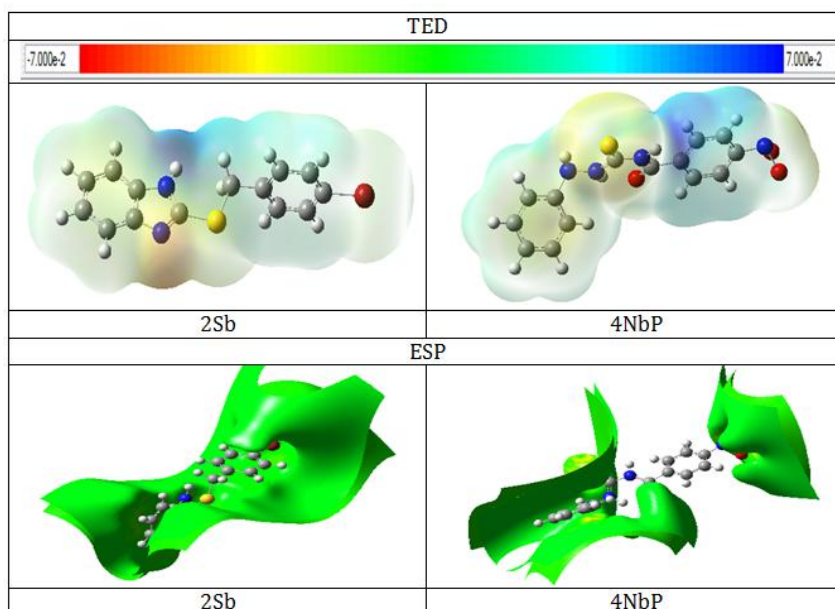
The studied inhibitors' native reactivity is investigated using the DFT Mulliken charges population analysis, which is an indication of reactive molecular centers (nucleophilic and electrophilic centers). The molecule counties where the electronic charge is large are therefore chemically softer than the regions where the electronic charge is small, so the electron density theaters play an essential role in the calculation of the chemical reactivity. In addition, chemical adsorption contacts are electrostatic or orbital interactions. In the molecule, the electrical charges measured the driving force of electrostatic interactions. However, charges are essential property in physicochemical reactions [24], it merely the charges for nitrogen (N), oxygen



(O), sulfur (S), and some carbon atoms are presented. Thus, the nucleophilic attack site will be the location where the negative charge value is the maximum. On the other side, the electrophilic attack site was controlled by the positive charge value of the most reactive sites that can accept electrons. The preferred sites for the electrophilic attack of 4NbP are therefore C13, C17, C18. The preferred electrophilic attack sites for 2Sb are C3, C9, C12, C15, N7. These atoms accept electrons from the metal atoms' 3d orbital to form feedback bonds, thus reinforcing the interaction between the metal surface and inhibitor. The favorite nucleophilic sites in 4NbP and 2Sb compounds, therefore, represent the atoms with negative charges. The attacking of the nucleophilic, should reactive spots that can donate electrons to metals. Table 3.7 shows the atomic charge for two inhibitors.

Depending on the above results, it can be decided that the two inhibitors have several functional centers for the adsorption on metal surfaces, such as (N, O, S) atoms and ring electrons, which donate electrons to metal surfaces for bonding. The S atom, however, can supply and receive the electron from metal because it has a single pair of electrons and unfilled d orbitals. Moreover, the active sites are the shape of a 2Sb molecule that is more planar than that of 4NbP Tables 3.1, 3.2, and Fig. 4. This

Table 6. Total electron density surface mapped with electrostatic potential of 2Sb and 4NbP molecules



makes it easier for 2Sb to be adsorbed by donating electrons to the metal surface.

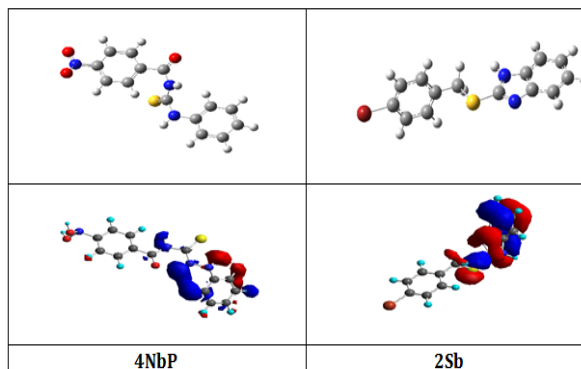


Figure 3. The Frontier Molecule Orbital density distributions of 4NbP, and 2Sb as calculated using the DFT method. Red color indicates the negatively charged lobe, and the blue color indicates the positive charge lobe.

In addition to, in figures of molecules, the active positions of the inhibitors molecule were further elaborated by the study of the molecular electrostatic potential (MEP), which was shown the electrons distribution and positions and charges density as a positive, negative and neutral zones on a defined color scale. The electrostatic surface potential (ESP) represents the direct adsorption centers of molecules onto the metal surface.

Table 7. DFT Mulliken charges population analysis for the calculated inhibitor molecules 4NbP and 2Sb.

Atom	Electronic Charge	Electronic charge	Atom	Electronic charge	Electronic charge
	2Sb	4NbP		2Sb	4NbP
C1	-0.285	-0.062	C17	-0.312	-0.084
C2	-0.212	0.234	Br18	-0.058	-
C3	0.548	-0.028	H19	0.119	-
C4	-0.080	0.043	H20	0.143	-
C5	-0.361	-0.047	H21	0.102	-
C6	-0.002	-0.086	H22	0.125	-
N7	0.075	-0.007	H23	0.202	0.074
N8	-0.369	-	H24	0.105	0.082
C9	0.402	-	H25	0.098	0.078
S10	-0.357	-	H26	0.122	0.067
C11	-0.108	-	H27	0.160	0.167
C12	0.645	0.308	H28	0.160	0.173
C13	-0.331	-	H29	0.123	-
C14	-0.363	-	N11	-	-0.314
C15	0.211	0.285	N14	-	-0.155
C16	-0.351	-0.074	C20	-	-0.064
C18	-	-0.064	S13	-	-0.323
H30	-	0.047	H33	-	0.061
H31	-	0.060	H34	-	0.051
H32	-	0.057	C10	-	0.547
C19	-	-0.009			
O8	-	-0.140			
O9	-	-0.140			
O21	-	-0.461			

Experimental Study

The two molecules were synthesized, and these compounds were diagnosed using IR spectrum and NMR spectrum. Used as a corrosion inhibitor to compare the two compounds as a corrosion inhibitor and determine the best where inhibition effectiveness was measured using a potentiostat and kinetic corrosion method such corrosion rate, E_a , ΔS^* and ΔH^* and thermodynamic activation parameters like E_a , ΔH_{ads} , and ΔS_{ads} by (OdayHadi) in Baghdad University. The two compounds are prepared as corrosion inhibitors, and the results show that the 2Sb inhibitor is more effective in inhibiting 4NbP inhibitors (94.11 IE percent) with less effective inhibition (13.21 IE percent) [33,34].

Conclusion

In this study, quantum mechanical calculations of PM3 and DFT (B3LYP) based on 6-311++G (2d,2p) were theoretically selected as better corrosion inhibitors. Physical properties and quantum chemical parameters were correlated with the inhibition efficiency of two inhibitors studied in the geometry of equilibrium. According to theoretical inhibition parameters, the inhibitor efficiency in the order of 2SB > 4NBP. The geometric structures showed that the reactive locations of the 2SB molecule were slightly more planar than 4NBP, making 2SB as a corrosion inhibitor more effective. The reactive site was calculated correctly by the DFT Mulliken charges for electrophilic and nucleophilic. These results were fixed



experimentally and proved to be theoretically suggested.

Acknowledgments

We acknowledge the support from the Eblal Initiative for Funding Scientific Research program.

References

- JP J. Stewart. Optimization of parameters for semiempirical methods V: modification of NDDO approximations and application to 70 elements. *J Mol Model* 2007; 13: 1173-1213.
- Stewart JJ. Optimization of parameters for semiempirical methods II. Applications. *Journal of computational chemistry* 1989; 10(2): 221-264.
- Stewart JJ. Optimization of parameters for semiempirical methods. III Extension of PM3 to Be, Mg, Zn, Ga, Ge, As, Se, Cd, In, Sn, Sb, Te, Hg, Tl, Pb, and Bi. *Journal of computational chemistry* 1991; 12(3): 320-341.
- Lewars E. *Computational chemistry. Introduction to the theory and applications of molecular and quantum mechanics* 2003.
- Gece G. The use of quantum chemical methods in corrosion inhibitor studies. *Corrosion science* 2008; 50(11): 2981-2992.
- Salman AW, Haque RA, Kadhim MM, Malan FP, Ramasami P. Novel triazine-functionalized tetra-imidazolium hexafluorophosphate salt: Synthesis, crystal structure and DFT study. *Journal of Molecular Structure* 2019; 1-6.
- Kubba RM, Khathem MM. Theoretical studies of corrosion inhibition efficiency of two new N-phenyl-ethylidene-5-bromo isatin derivatives. *Iraqi Journal of Science* 2016; 57(2B):1041-1051.
- Anaee RA, Tomi IHR, Abdulmajeed MH, Naser SA, Kathem MM. Expired Etoricoxib as a corrosion inhibitor for steel in acidic solution. *Journal of Molecular Liquids* 2019;279: 594-602.
- Al-Fahemi JH, Abdallah M, Gad EA, Jahdaly BAAL. Experimental and theoretical approach studies for melatonin drug as safely corrosion inhibitors for carbon steel using DFT. *Journal of Molecular Liquids* 2016; 222: 1157-1163.
- Prabha SS, Rathish RJ, Dorothy R, Brindha G, Pandiarajan M, Al-Hashem A, Rajendran S. Corrosion problems in petroleum industry and their solution. *European Chemical Bulletin* 2014; 3(3), 300-307.
- Yaqo EA, Anaee RA, Abdulmajeed MH, Tomi IH, Kadhim MM. Aminotriazole Derivative as Anti-Corrosion Material for Iraqi Kerosene Tanks: Electrochemical, Computational and the Surface Study. *Chemistry Select* 2019; 4(34): 9883-9892.
- Al-Majidi SMH, Hama LHK. Synthesis and antimicrobial evaluation activity of some new substituted spiro-thiazolidine, imidazolinone and azetidione derivatives of 5-bromo isatin. *Journal of Zankoi Sulaimani* 2015;17(1):49-59.
- Luo H, Guan YC, Han KN. Inhibition of mild steel corrosion by sodium dodecyl benzene sulfonate and sodium oleate in acidic solutions. *Corrosion* 1998; 54(8): 619-627.
- Quraishi MA, Jamal D. Corrosion inhibition by fatty acid oxadiazoles for oil well steel (N-80) and mild steel. *Materials chemistry and physics* 2001; 71(2): 202-205.
- Ma H, Chen S, Yin B, Zhao S, Liu X. Impedance spectroscopic study of corrosion inhibition of copper by surfactants in the acidic solutions. *Corrosion Science* 2003; 45(5): 867-882.
- Issa RM, Awad MK, Atlam FM. Quantum chemical studies on the inhibition of corrosion of copper surface by substituted uracils. *Applied Surface Science* 2008; 255(5): 2433-2441.
- Vračar LM, Dražić DM. Adsorption and corrosion inhibitive properties of some organic molecules on iron electrode in sulfuric acid. *Corrosion Science* 2002; 44(8):1669-1680.
- Abboud Y, Abourriche A, Saffaj T, Berrada M, Charrouf M, Bennamara A, Takky D. The inhibition of mild steel corrosion in acidic medium by 2, 2'-bis (benzimidazole). *Applied surface science* 2006; 252(23): 8178-8184.
- Khaled KF. The inhibition of benzimidazole derivatives on corrosion of iron in 1 M HCl solutions. *Electrochimica Acta* 2003; 48(17):2493-2503.
- Koopmans T. Über die Zuordnung von Wellenfunktionen und Eigenwerten zu den einzelnen Elektronen eines Atoms. *Physica* 1934; 1(1-6):104-113.
- Parr RG, Pearson RG. Absolute hardness: companion parameter to absolute electronegativity. *Journal of the American chemical society* 1983; 105(26):7512-7516.
- Chermette H. Chemical reactivity indexes in density functional theory. *Journal of Computational Chemistry* 1999; 20(1): 129-154.
- Lukovits I, Kalman E, Zucchi F. Corrosion inhibitors—correlation between electronic structure and efficiency. *Corrosion* 2001; 57(1): 3-8.
- Wang H, Wang X, Wang H, Wang L, Liu A. DFT study of new bipyrazole derivatives and their potential activity as corrosion inhibitors. *Journal of Molecular Modeling* 2007;13(1):147-153.
- Kubba RM, Abood FK. Quantum Mechanical Calculations for Some PINH Cs Symmetry Schiff Bases as Corrosion Inhibitors for Mild Steel. *Iraqi Journal of Science* 2015; 56(2B):1241-1257.
- Ebenso EE, Isabirye DA, Eddy NO. Adsorption and quantum chemical studies on the inhibition potentials of some thiosemicarbazides for the corrosion of mild steel in acidic medium. *International journal of molecular sciences* 2010; 11(6): 2473-2498.
- Ahamad I, Prasad R, Quraishi MA. Thermodynamic, electrochemical and quantum chemical investigation of some Schiff bases as corrosion inhibitors for mild steel in hydrochloric acid solutions. *Corrosion Science* 2010; 52(3):933-942.
- Sonawane RP, Tripathi RR. The chemistry and synthesis of 1H-indole-2, 3-dione (Isatin) and its derivatives. *International Letters of Chemistry, Physics and Astronomy* 2013;7(1):30-36.
- Bentiss F, Lebrini M, Lagrenée M. Thermodynamic characterization of metal dissolution and inhibitor adsorption processes in mild steel/2, 5-bis (n-thienyl)-1, 3, 4-thiadiazoles/hydrochloric acid system. *Corrosion Science* 2005; 47(12):2915-2931.



Khalil, N. (2003). Quantum chemical approach of corrosion inhibition. *Electrochimica Acta* 2003; 48(18):2635-2640.

Zhao P, Liang Q, Li Y. Electrochemical, SEM/EDS and quantum chemical study of phthalocyanines as corrosion inhibitors for mild steel in 1 mol/l HCl. *Applied Surface Science* 2005; 252(5):1596-1607.

Obot IB, Obi-Egbedi NO. Theoretical study of benzimidazole and its derivatives and their potential activity as corrosion inhibitors. *Corrosion Science* 2010; 52(2):657-660.

Al-Majidi SM, Al-Jeilawi UH, Khulood AS. Synthesis and characterization of some 2-sulphonyl benzimidazole derivatives and study of effect as corrosion inhibitors for carbon steel in sulfuric acid solution. *Iraqi Journal of Science* 2013; 54(4):789-802.

Oday H. Synthesis of some organic compounds as corrosion inhibition in petroleum industry. Baghdad: Baghdad University 2013.